Available online at www.sciencedirect.com
ScienceDirect
Journal of Solid State Chemistry 180 (2007) 3234–3246
JOURNAL OF SOLID STATE CHEMISTRY
www.elsevier.com/locate/jssc

# Atomic and vacancy ordering in carbide ζ-$Ta_4C_{3-x}$ ($0.28 \leqslant x \leqslant 0.40$) and phase equilibria in the Ta–C system

A.I. Gusev*, A.S. Kurlov, V.N. Lipatnikov

*Institute of Solid State Chemistry, Ural Division of the Russian Academy of Sciences, 620041 Yekaterinburg, Russian Federation*

Received 29 June 2007; received in revised form 11 September 2007; accepted 15 September 2007
Available online 21 September 2007

**Abstract**

The structure of nonstoichiometric carbide phase ζ-$Ta_4C_{3-x}$ formed in the tantalum–carbon (Ta–C) system is studied by X-ray and neutron powder diffraction and metallography. Investigated carbide ζ-$TaC_{0.67}$ crystallizes in a trigonal (rhombohedral) space group $R\bar{3}m$ with cell parameters $a_{tr} = 1.0180(1)$ nm, $\alpha_{tr} = 17.64^\circ$ (or $a_h = 0.31216(2)$ nm, $c_h = 3.0058(1)$ nm in hexagonal axes). The closely packed metal sublattice in carbide ζ-$Ta_4C_{3-x}$ consists of alternating blocks where metal atoms are located in the same manner as on the FCC sublattice of the cubic carbide $TaC_y$ and the HCP sublattice of the hexagonal carbide $Ta_2C_y$. This metal sublattice represents a transition sublattice between these FCC and HCP sublattices. An ordered distribution of atoms C and structural vacancies in carbide ζ-$Ta_4C_{3-x}$ is revealed and the distribution function of atoms C is calculated for nonmetal sublattice sites, on which ordering takes place. It is shown that one long-range order parameter η describes the ordering of ζ-carbide and the η value in the investigated ζ-$Ta_4C_{3-x}$ phase does not exceed 0.7. Carbide ζ-$Ta_4C_{3-x}$ is stable in bulk and powdered states over a wide temperature interval of 300 to ~2400 K and has a narrow homogeneity interval from $TaC_{0.65}$ to $TaC_{0.68}$. Microhardness of disordered and ordered tantalum carbide $TaC_y$ with the basic $B1$ structure and trigonal carbide ζ-$Ta_4C_{3-x}$ is measured. The phase diagram of the Ta–C system is refined considering data obtained for the ζ-$Ta_4C_{3-x}$ phase.


*Keywords:* Tantalum carbide; Vacancy ordering; Phase diagram of the Ta–C system

## 1. Introduction

A characteristic feature of cubic $MC_y$ ($MC_y\square_{1-y}$, 0.65–0.70 $\leqslant y \leqslant$ 0.88–1.00) and hexagonal $M_2C_{y'}$ ($MC_{y'/2}\square_{0.5-y'/2}$, $0.70 < y' \leqslant 1.00$) carbides of binary $M$–C systems ($M$ = V, Nb, Ta) of group V transition metals with carbon (C), is a high nonstoichiometry of the nonmetal sublattice. The same feature is inherent in trigonal (rhombohedral) ζ-$M_4C_{3-x}$ ($M_4C_{3-x}\square_{1+x}$ or $MC_{(3-x)/4}\square_{(1+x)/4}$, $0.20 < x < 0.50$) carbides of vanadium, niobium and tantalum (Ta). The content of structural vacancies □ in the carbon sublattice of ζ-carbides may amount to tens of atomic %. Cubic, hexagonal and trigonal carbides are included in the group of strongly nonstoichiometric compounds [1,2]. A large concentration of structural vacancies in nonstoichiometric carbides is a premise of their atomic and vacancy ordering. Ordering in cubic $MC_y$ and hexagonal $M_2C_{y'}$ carbides has been studied in detail both experimentally and theoretically [1,2]. Ordering of nonstoichiometric ζ-carbides, which are known in the literature as ζ-$M_4C_{3-x}$ phases with a trigonal basic lattice, has been just guessed.

The ζ-phase was first detected in two- and three-phase samples of the Ta–C system over the interval of compositions between hexagonal $TaC_{0.52}$ and cubic $TaC_{0.73}$ carbides [3]. The content of the ζ-phase was a maximum in $TaC_{0.59-0.64}$ carbides. When $TaC_{0.64}$ carbide was heated at 2070 K for 26 h, the relative concentration of the ζ-phase increased, but the sample still was a three-phase compound. Heating of the sample at a higher temperature was followed by the decrease in the phase concentration and smearing of ζ-phase reflections in the X-ray diffraction (XRD) pattern. Later the ζ-phase was observed in Hf–Ta–C and Ta–B–C ternary systems [4,5]. The ζ-phase composition was defined as $Ta_3C_2$ by Rudy et al. [4,5]. The researchers [6–9] studied diffusion saturation of metallic Ta

*Corresponding author.
*E-mail address:* gusev@ihim.uran.ru (A.I. Gusev).

0022-4596/$ - see front matter © 2007 Elsevier Inc. All rights reserved.
doi:10.1016/j.jssc.2007.09.015

with carbon and found that the ζ-phase precipitated in the gap between layers of nonstoichiometric cubic $TaC_y$ and hexagonal $Ta_2C$ carbides.

An X-ray analysis of ζ-phases of vanadium, niobium and tantalum carbides [10] demonstrated that ζ-phases have the trigonal (space group $R\bar{3}m$) symmetry and their composition can be written as $M_4C_{3-x}$. Carbon atoms in ζ-$M_4C_{3-x}$ phases ($M = V$, Nb, Ta) are located in octahedral interstices of the closely packed metal sublattice. The lattice constants of ζ-$Ta_4C_3$ carbide of unknown composition are equal to $a = 0.3116$ and $c = 3.000$ nm in hexagonal axes [10]. The electron diffraction [11] from the ζ-$Ta_4C_{3-x}$ phase, which was prepared through diffusion saturation of a Ta foil with carbon, showed that the ζ-phase belongs to the structural type $Sn_2P_3$ (space group $R\bar{3}m$) and its composition should approach $TaC_{0.67}$. This composition is realized thanks to a large concentration of carbon vacancies concerning the stoichiometric composition $Ta_4C_3$: the maximum $x$ value in ζ-$Ta_4C_{3-x}$ can be as large as 0.4–0.5. Considering results of the electron microscopy examination of cubic (with the $B1$ structure) $TaC_{0.70}$–$TaC_{0.80}$ carbides, it was supposed [12] that the ζ-phase was formed from nonstoichiometric cubic $TaC_y$ carbide as a result of removal of every 4th carbon plane $(111)_{B1}$ and the corresponding shift of the metal atomic planes $(111)_{B1}$.

The diffraction reflection intensities of the ζ-phase, which are reported in the literature, considerably differ and, therefore, its structure has not been ascertained so far. The formation of ζ-$Ta_4C_{3-x}$ is erroneously referred by authors [13,14] to as ordering of cubic carbide $TaC_y$. However, the described phase transformation is not a disorder–order transition between disordered cubic carbide $TaC_y$ and trigonal carbide ζ-$Ta_4C_{3-x}$ since the metal sublattice in ζ-carbide has a hexagonal no cubic symmetry. According to experimental data [15], the ζ-$Ta_4C_{3-x}$ phase contains 38.2–39.0 at% C, is formed by a peritectoid reaction at a temperature below 2450 K, and exists in the equilibrium state over the temperature interval from ~1440 to ~2450 K. If $T < 1400$ K, the metastable steady state of the ζ-$Ta_4C_{3-x}$ phase may be maintained by quenching.

The conclusion [15] about a limited interval of the thermal stability of ζ-$Ta_4C_{3-x}$ contradicts the experimental data [16,17]. Tantalum carbide samples [16,17] were prepared by the gas-phase diffusion deposition of Ta onto a graphite substrate and contained ~80% of ζ-$Ta_4C_{3-x}$. The analysis of the phase composition of carbide samples [16] showed that the ζ-$Ta_4C_{3-x}$ phase was stable during annealing in a vacuum or an Ar atmosphere over a wide temperature interval of 300–3170 K. The authors [16] believe that the conclusions [7,8,13,14] about the metastability of the ζ-$Ta_4C_{3-x}$ phase were drawn because in the latter studies the ζ-phase was obtained in a nonequilibrium state. Indeed, the data [7,8,15] on the position of phase boundaries, which were determined by means of diffusion couples, are not equilibrium since the sample has a concentration gradient of the components over its cross-section. Thus, conclusion concerning the position of ζ-phase boundaries, which follow from results of the diffusion couples method, may prove to be not quite correct. A high pressure, which was used [13,14] for synthesis of tantalum carbides, also could displace the boundaries of the homogeneity interval of ζ-$Ta_4C_{3-x}$ phase and, hence, lead to synthesis of a nonequilibrium ζ-phase, which decomposed upon heating or grinding.

A large (25–33–35 at%) concentration of structural vacancies in the carbon sublattice of the ζ-$Ta_4C_{3-x}\square_{1+x}$ carbide phase is a prerequisite of possible atomic-vacancy ordering. There have been no experimental evidences in favor of a disordered (statistical) or ordered distribution of carbon atoms and vacancies for a long time. The scattering amplitude of X-ray radiation by C atoms is much smaller than that by Ta atoms. Therefore, in the XRD experiment with ζ-$Ta_4C_{3-x}$ carbide the relative change of the reflection intensity caused by the redistribution of atoms C is very small. If a sample contains impurity other carbide phases and, what is more, is textured (both features are characteristic of samples with the ζ-phase), a disordered or ordered distribution of carbon atoms and vacancies cannot be determined by the XRD. The problem of the distribution of carbon atoms and structural vacancies in ζ-$Ta_4C_{3-x}$ can be solved experimentally using neutron diffraction. Studying of ζ-$Ta_4C_{3-x}$ [18] by this method revealed that the intensity ratio of some diffraction reflections is characteristic for the ordered distribution of carbon atoms C and vacancies □. However, no refinement of structure of the ζ-$Ta_4C_{3-x}$ phase was performed by authors [18] and the structure of the ordered phase has not been determined in detail.

The aim of the present work was to study and refine the crystal structure of ζ-$Ta_4C_{3-x}$ phase, to determine the disorder–order phase transition channel and to analyze the distribution of atoms C and vacancies □ in the ζ-$Ta_4C_{3-x}$ lattice, to construct the phase diagram of the Ta–C system taking into account the presence of ζ-phase and to obtain information about the effect of nonstoichiometry on the microhardness of cubic and trigonal tantalum carbides.

## 2. Samples and experiment

The starting materials for the preparation of samples containing ζ-$Ta_4C_{3-x}$ phase were Ta powder with particles 3–5 μm in size and purity of 99.9%, carbon black with purity of 99.999% and powders of $TaC_{0.975}$ and $TaC_{0.75}$ cubic carbides synthesized previously in [19]. The starting tantalum carbides powders contained the following impurities (wt%): $10^{-4}$ V, $10^{-4}$ Zr, $10^{-3}$ Nb, $10^{-4}$ Ni, $10^{-3}$ Mg, 0.12 O, and 0.05 N.

Samples of tantalum carbide $TaC_{0.68}$–$TaC_{0.78}$ were synthesized by solid-phase sintering of powder mixtures in a vacuum of 0.0013 Pa ($10^{-5}$ mm Hg) under three different temperature routes: (I) sintering of the mixture of $TaC_{0.975}$ and Ta for 6 h at a temperature of 2270 K with intermediate grinding of the products after 3 h of sintering;

(II) sintering of the mixture of $TaC_{0.75}$ and C or $TaC_{0.75}$ and Ta for 6 h at 2300–2400 K with intermediate grinding of the products after 3 h of sintering; (III) sintering of the mixture of $TaC_{0.75}$ and C or $TaC_{0.75}$ and Ta for 20 h at a temperature of 2300–2400 K with intermediate grinding after 10 h of sintering. Chemical analysis of tantalum carbides for carbon and nitrogen was carried out by Dumas gas chromatography on a Carlo Erba CHN 1108 analyser. The oxygen content of the starting powders and of the samples was measured by a vacuum hot extraction equipment Balzers exhalograph EAO-201. The metal impurity content of the starting powders and of the sintered samples was determined by inductively coupled plasma-mass spectrometry on a Spectromass 2000. The surface composition of the sintered samples was studied by EDX method on a JEOL 6310 scanning electron microscope with an integrated EDX apparatus. Relative content of carbon, $y$, in $TaC_y$ carbides was determined with an accuracy of $\pm 0.003$.

All the XRDs were collected at angles $2\theta$ from 5 to 120° with a step of $\Delta(2\theta) = 0.02°$ by the Bragg–Brentano method in the Cu$K\alpha_{1,2}$ radiation and the Guinier method in the Cu$K\alpha_1$ radiation using a STADI-P (STOE) transmission-geometry diffractometer. Polycrystalline silicon with lattice constant $a = 0.543075(5)$ nm was used as external standard. The phase content of the samples was checked in an optical microscope in polarized light and by comparing their XRD patterns with those in the PDF2 database (powder diffraction file, ICDD, USA) release 2002. Neutron diffraction data were collected with the $D7A$ neutron diffractometer at the research water–water atomic reactor IVV-2M (Zarechny, Russia). Neutron diffraction measurements were performed with the use of a beam of neutrons of wavelength $\lambda = 0.1532 \pm 0.0002$ nm; the diffractometer resolution $\Delta d/d$ was equal to 0.01. Neutron diffraction patterns were recorded at room temperature in a step-scanning mode with steps of $\Delta(2\theta) = 0.1°$ and an exposure time of 60 s at each point within the region $2\theta$ from 10° to 125°. The crystal structure was determined with the program EXPO [20] and the final refinements from powder data were carried out with the GSAS program package [21]. Background was fitted by the Chebyshev 6th-order polynomial. The reflection shape was modeled as a pseudo-Voigt function.

Metallographic sections for analysis of the microstructure and measurements of the microhardness were prepared in a metallographic complex including PNEUMET-2, MOTOPOL-8 and MICROMET-1 instruments. For exposure of grain boundaries the polished microsections were etched in an acid mixture ($2HNO_3 + 6HF + 3H_2O$). The microstructure of the samples was examined in reflected polarized white light using a Neophot-2 optical polarization microscope (Carl Zeiss Jena) at a magnification of 100–1000 power. The microhardness $H_V$ was measured by the Vickers method using a MICROMET-I microhardness testing machine with automatic loading. The load was 0.1 kg and the loading time was 10 s.

## 3. Structure of the ζ-$Ta_4C_{3-x}$ phase and carbon atom distribution

### 3.1. Chemical and structure characterization

The $TaC_{0.685}$ sample, which was synthesized under the first route, included a large quantity of ζ-$Ta_4C_{3-x}$. The ζ-phase was absent in the as-synthesized samples prepared under the routes (II) and (III). Therefore they were annealed additionally. The samples synthesized under conditions (II) were annealed at 1470 K for 100 h and then the annealing temperature was decreased to 570 K at a rate of 0.25 K $min^{-1}$. The samples synthesized under conditions (III) were annealed at 1570 K for 35 h, then the annealing temperature was reduced to 1170 K during 120 h, and finally it was decreased to 570 K at a rate of 0.25 K $min^{-1}$. Intense reflections of the ζ-$Ta_4C_{3-x}$ phase appeared in XRDs of the annealed bulk samples of $TaC_{0.70}$ and $TaC_{0.72}$ carbides. Some authors [7,14] report vanishing of the ζ-phase after grinding of bulk samples. However, this effect was not observed in the present study: reflections of the ζ-phase are preserved in XRD patterns of the powders prepared by grinding of $TaC_{0.685}$, $TaC_{0.70}$ and $TaC_{0.72}$ bulk samples.

The chemical composition and the content of Ta, bound (chemically combined) carbon $C_{bound}$ and gas impurities in the tantalum carbide samples investigated are given in Table 1; no free (chemically uncombined) carbon $C_{free}$ was found. The presence of Ta, C and impurity metallic Mg (Fig. 1) was detected by EDX method on the surface of sintered bulk and powdered samples of $TaC_{0.685}$ containing a large amount of ζ-$Ta_4C_{3-x}$. The reason for the presence of Mg traces is the following fact. In comparison with transition metals, magnesium does not to replace Ta atoms in the metallic sublattice of tantalum carbide. Therefore, high-temperature sintering leads to appearance of Mg on the sample surface owing to the surface segregation of this admixture. The total impurity content of the samples did not exceed 0.25 wt%.

A specific feature of the XRD and neutron diffraction patterns obtained by the Bragg–Brentano method both for powder and bulk samples is a large intensity of the

Table 1
Chemical and phase composition of $TaC_y$ samples

| $TaC_y$ samples | Content (wt%) | | | | Phases |
|---|---|---|---|---|---|
| | Ta ±0.1 | $C_{bound}$[a] ±0.03 | O ±0.01 | N ±0.01 | |
| $TaC_{0.685}$ | 95.5 | 4.34 | 0.12 | 0.03 | ζ-$Ta_4C_{3-x}$, $TaC_y$, $Ta_2C$ |
| $TaC_{0.70}$ | 95.4 | 4.43 | 0.16 | 0.04 | ζ-$Ta_4C_{3-x}$, $TaC_y$, $Ta_2C$ |
| $TaC_{0.72}$ | 95.2 | 4.54 | 0.14 | 0.05 | ζ-$Ta_4C_{3-x}$, $TaC_y$, $Ta_2C$ |
| $TaC_{0.75}$ | 95.1 | 4.74 | 0.15 | 0.06 | $TaC_y$ |
| $TaC_{0.76}$ | 95.1 | 4.79 | 0.14 | 0.03 | $TaC_y$ |
| $TaC_{0.78}$ | 95.0 | 4.92 | 0.19 | 0.04 | $TaC_y$ |

[a]Free carbon $C_{free}$ is absent.

reflections (0012) and (0024), which is several times higher than their theoretical intensity. A multiple increase in the intensity of these reflections is due to axial texturing of the samples in the direction (00*l*), i.e. along the *c*-axis of the ζ-phase. Indeed, the analysis of the microstructure of bulk tantalum carbide samples revealed characteristic strongly textured lamellar precipitates of the ζ-$Ta_4C_{3-x}$ (Fig. 2). An analogous microstructure of samples with the ζ-phase was observed earlier [7,8,11,12,14].

A large effect of the texture of ζ-$Ta_4C_{3-x}$ samples on the intensity of XRD reflections was noted by authors [7,17,18]. Considerable difference of relative intensities of diffraction reflections of the ζ-phase [3,7,14,17] are just due to a larger or smaller axial texture. In order to exclude the effect of the texture on the reflection intensity, the XRD patterns were collected using a Guinier method with a large accumulation of signals at each point. Thanks to the precision measurements, the signal-to-noise ratio was very high against a sufficiently low background. It was 30–40 for medium-intensity reflections and 70–80 for most intense reflections (the signal-to-noise ratio was not over 20 for medium lines in the case of the standard procedure with the same $TaC_y$ samples). The survey made by a Guinier method weakened significantly the effect of the texture on the intensity of diffraction reflections. The use of Cu$K\alpha_1$ radiation eliminated doublet reflections and, hence, improved the measurement accuracy.

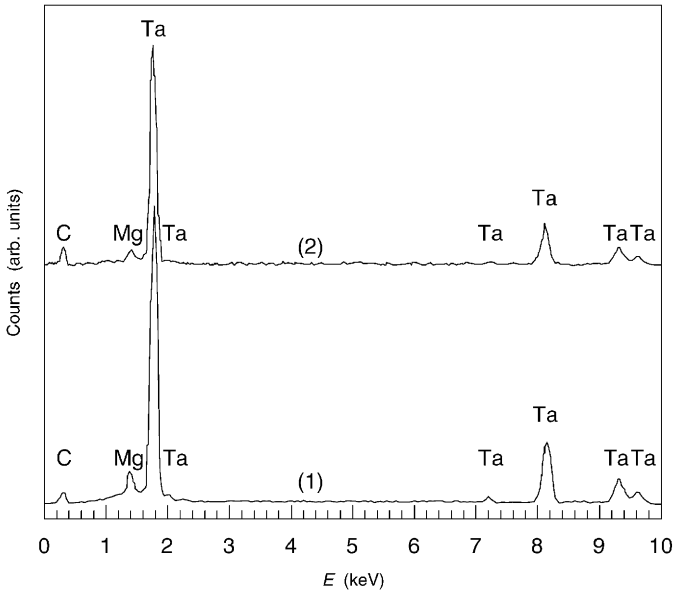


Fig. 1. EDX spectra of the surface of an individual grain (1) of the ζ-$Ta_4C_{3-x}$ phase and the textured surface (2) of a sintered $TaC_{0.685}$ sample containing ~75 wt% of the ζ-$Ta_4C_{3-x}$ phase. Traces of impurity magnesium Mg along with tantalum (Ta) and carbon (C) are present on the surface.

Diffraction study showed that all the samples of tantalum carbide with the ζ-phase contained also cubic carbide $TaC_y$ with the *B*1 structure and a small quantity of hexagonal carbide $Ta_2C$ with the *L*′3 structure. Phase composition of all samples was determined from XRD patterns. The $TaC_{0.685}$ sample contained ~20, ~5 and ~75 wt% of cubic carbide $TaC_y$, hexagonal lower carbide $TaC_{0.50}$ ($Ta_2C$) and the ζ-phase, respectively. Another sample $TaC_{0.70}$ contained ~35, ~2 and ~63 wt % of $TaC_y$, $TaC_{0.50}$ ($Ta_2C$) and the ζ-phase. The $TaC_{0.72}$ sample contained about 53, 2 and 45 wt% of $TaC_y$, $TaC_{0.50}$ ($Ta_2C$) and the ζ-phase, respectively.

The presence of three phases $TaC_y$, $Ta_2C_y$ and ζ-$Ta_4C_{3-x}$ in $TaC_{0.685}$ sample produced by sintering at 2300 K points out that the sample chemical composition and the sintering temperature are close to the point of a peritectoid formation of ζ-phase. The as-synthesized samples $TaC_{0.70}$ and $TaC_{0.72}$ contained 75 wt% of cubic $TaC_y$ and 25 wt% of hexagonal $Ta_2C_y$ carbides. After prolonged low-temperature annealing ζ-phase appeared, content of cubic carbide decreased by a factor of nearly 2 and content of hexagonal carbide decreased up to ~2 wt% in those samples. Obviously, annealing duration was not enough for reaching of equilibrium state in which samples contain only two phases ζ-$Ta_4C_{3-x}$ and $TaC_y$. Note that three-phase samples containing cubic and hexagonal carbides along with ζ-$Ta_4C_{3-x}$ were obtained in previous studies [3,6–9,13,14].

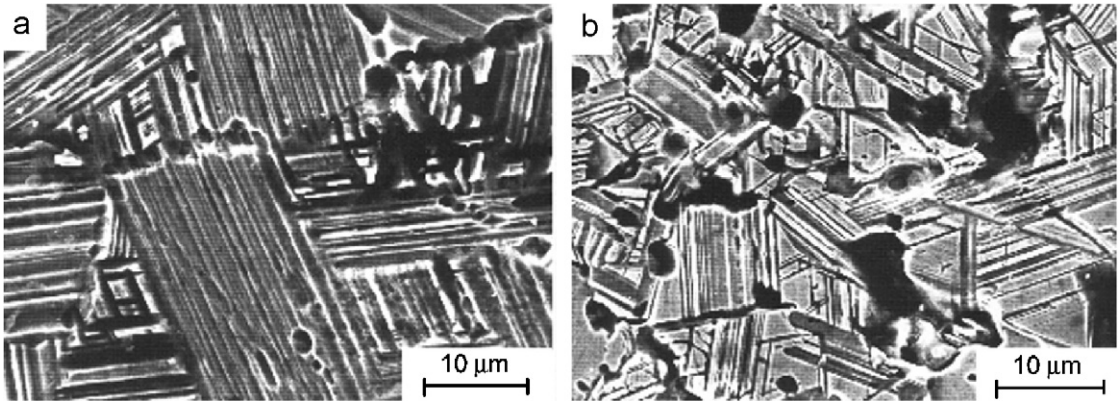


Fig. 2. Microstructure of sintered samples of $TaC_{0.685}$ (a) and $TaC_{0.72}$ (b) with lamellar precipitates of the ζ-$Ta_4C_{3-x}$ phase. The samples are strongly textured. This microstructure is characteristic of all the tantalum carbide samples containing the ζ-phase.

Analysis performed suggests that the set of diffraction reflections from the $\zeta$-$Ta_4C_{3-x}$ phase, which is observed in the XRD pattern, corresponds to a trigonal (space group $R\bar{3}m$) unit cell. The unit cell of the $\zeta$-phase contains three formula units $Ta_4C_{3-x}$.

Parameters of unit cells of the observed phases and the phase composition of the $TaC_{0.685}$ sample were determined from XRD patterns. The unit cell lattice constants of the trigonal (space group $R\bar{3}m$) $\zeta$-$Ta_4C_{3-x}$ phase are $a_h = 0.31216(2)$ and $c_h = 3.0058(1)$ nm. The known relationships $\sin(\alpha_{tr}/2) = 1.5/\sqrt{3 + (c_h/a_h)^2}$ and $a_{tr} = c_h/\sqrt{9 - 12\sin^2(\alpha_{tr}/2)}$ were used for conversion from the hexagonal parameters $a_h$ and $c_h$ to the trigonal parameters $a_{tr}$ and $\alpha_{tr}$ of the unit cell. The unit cell parameters in the trigonal axes are equal to $a_{tr} = 1.0180(1)$ nm and $\alpha_{tr} = 17.64^\circ$. The lattice constant of the cubic (space group $Fm\bar{3}m$) phase is $a_{B1} = 0.44188(1)$ nm and corresponds to the carbide $TaC_{0.765}$. The lattice constants of the hexagonal (space group $P6_3/mmc$) carbide $Ta_2C$ are $a = 0.3116(1)$ and $c = 0.4886(4)$ nm. Considering the composition of the samples and content of cubic $TaC_{0.765}$ and hexagonal $TaC_{0.50}$ ($Ta_2C$) carbides in the samples, the composition of $\zeta$-phase investigated corresponds to $\sim TaC_{0.68-0.67}$ ($\sim TaC_{2/3}$) or $Ta_4C_{3-x}$ with $x \approx 0.28$–$0.32$.

According to [10] in the perfect trigonal $\zeta$-$M_4C_{3-x}$ carbide structure 12 metal atoms occupy twice the positions 6($c$) with the coordinates $(00\frac{1}{8})$ and $(00\frac{7}{24})$, while the nonmetal sublattice sites are in positions 3($a$), 3($b$) and 6($c$) with the coordinates (000), $(00\frac{1}{2})$ and $(00\frac{5}{12})$, respectively (here and further the atomic coordinates and parameters of a unit cell are given in hexagonal axes). One-quarter of all sites in the nonmetal sublattice are vacant in $\zeta$-$M_4C_{3-x}\square_{1+x}$ phases even at $x = 0$. It is known that carbon atoms fully occupy positions 6($c$) and the remaining atoms C and vacancies are located in positions 3($a$) and 3($b$). Atoms C and vacancies $\square$ can have a statistical or ordered distribution over positions 3($a$) and 3($b$). In the case of the statistical distribution, atoms C occupy positions 3($a$) and 3($b$) in the nonmetal sublattice with an equal probability $(1-x)/2$. Two variants of the ordered distribution are possible. In the first variant, carbon atoms occupy positions 3($a$) with a probability $(1-x)$, while positions 3($b$) are vacant. In the second variant, atoms C are in positions 3($b$) with a probability $(1-x)$ and positions 3($a$) are vacant. Since new crystallographic positions are not formed in the case of this ordering, the lattice symmetry is preserved and just a redistribution of the reflection intensity will be observed in the diffraction patterns. No additional reflections will appear.

The refinement of structure was performed for $TaC_{0.685}$ carbide powder with using of the XRD patterns obtained by a Guinier method. Observed $I_{obs}$, calculated $I_{calc}$ and difference ($I_{obs} - I_{calc}$) values corresponding to the refinement of the XRD pattern for $TaC_{0.685}$ powder are shown in Fig. 3. The satisfactory agreement between the experimental and calculated diffraction data ($R_I = 0.0867$) was attained for the XRD pattern made by a Guinier method (Fig. 3); for the XRD pattern made by the Bragg–Brentano method, the realibility factor $R_I$ equals 0.1296. The intensity ratio of the observed XRD reflections from the

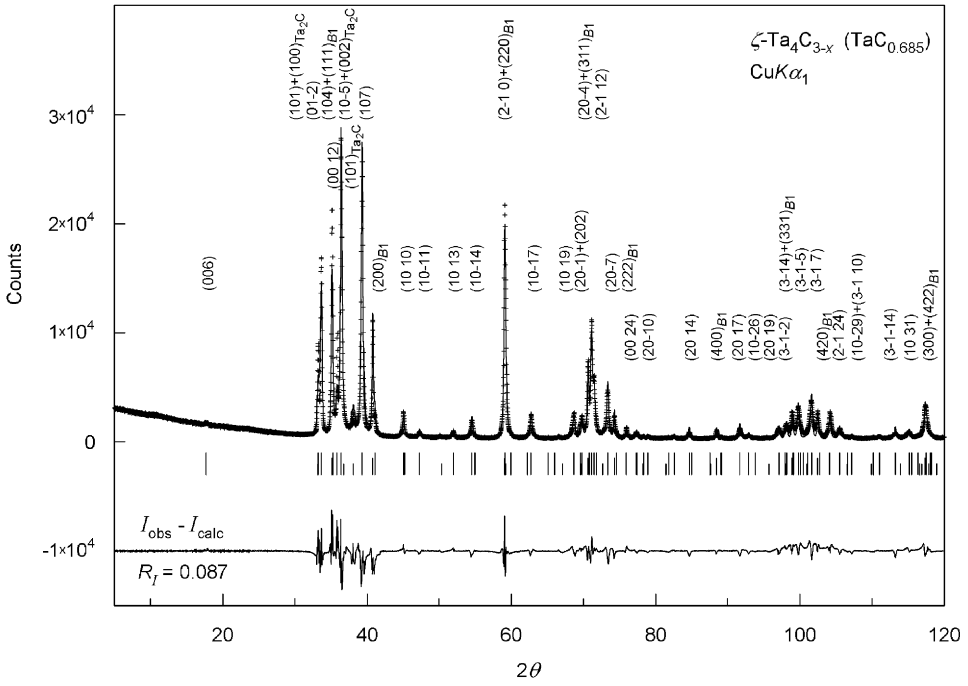


Fig. 3. Observed (crosses), calculated (solid line) and difference XRD patterns for $TaC_{0.685}$ powder containing ~75 wt% of the $\zeta$-$Ta_4C_{3-x}$ phase (Guinier method, Cu$K\alpha_1$ radiation). Long, middle and short ticks correspond to reflections of $\zeta$-$Ta_4C_{3-x}$, $TaC_{0.76}$ and $Ta_2C$ phases, respectively.

Table 2
Crystal data, experimental conditions and characteristics of the refinement for the ζ-$Ta_4C_{3-x}$ carbide

| | | |
|---|---|---|
| Chemical formula | $Ta_4C_{8/3}$ | |
| Formula weight | 755.82 | |
| Crystal system | Trigonal | |
| Space group | $R\bar{3}m$ (no. 166) | |
| $a$ (nm) | 0.31216(3) | |
| $b$ (nm) | 0.31216(3) | |
| $c$ (nm) | 3.0058(1) | |
| $Z$ | 3 | |
| $V$ ($nm^3$) | 0.253657 | |
| $D_{calc}$ ($g\,cm^{-3}$) | 14.84 | |
| Diffractometer | STADI-P | *D*7A |
| Radiation type | X-ray Cu$K\alpha_1$ | Neutrons |
| Wavelength (nm) | 0.154056 | 0.153208 |
| $2\theta$ Range (°) | 5–120 | 10–125 |
| Step-scan (°) | 0.02 | 0.1 |
| Counting time (s) | 20 | 60 |
| Preferred orientation | (001) | (001) |
| $R_I$ ($R_{Bragg}$) (%) | 8.67 | 5.95 |
| $R_p$ (%) | 12.87 | 9.94 |
| w$R_p$ (%) | 15.25 | 12.79 |
| $R_{exp}$ (%) | 9.22 | 4.90 |

ζ-phase corresponds either to the statistical (disordered) distribution of carbon atoms on sites 3(*a*) and 3(*b*) in the nonmetal sublattice or to the ordered distribution when carbon atoms occupy positions 3(*a*), while positions 3(*b*) are vacant. One more variant of ordering when atoms C are located in positions 3(*b*) and vacancies occupy positions 3(*a*) disagrees with the experimental data. Details of the structure refinement of the ζ-$Ta_4C_{3-x}$ phase are given in Table 2. The determination of coordinates taking into account displacements of atoms provided indirect information about the distribution of atoms C and vacancies □.

According to refinement results, in a unit cell of the ζ-$Ta_4C_{3-x}$ phase positions 6(*c*) with the coordinates (0, 0, 0.1273(6)) and (0, 0, 0.291(10)) are occupied twice by twelve atoms Ta, positions 6(*c*) with the coordinates (0, 0, 0.4169(9)) are occupied by carbon atoms. Positions 3(*a*) and 3(*b*) with the coordinates (000) and $(00\frac{1}{2})$ correspond to lattice sites, on which the distribution of atoms C can be disordered or ordered (Fig. 4). It is seen that atomic displacements from the positions of ideal trigonal structure are rather large. Atoms Ta, which occupy positions 6(*c*) with the coordinates (0 0 0.1273(6)) in planes perpendicular to the *c*-axis of the unit cell, are displaced to the carbon sublattice planes formed by sites 3(*b*) and from the carbon sublattice planes formed by sites 3(*a*) (see Fig. 4(1)). These displacements provide indirect evidence to different occupancies of positions 3(*a*) and 3(*b*) by atoms C, i.e. point to their probable ordering. In the disordered ζ-$Ta_4C_{3-x}$ phase, spacings between metal plane should be equal one another along the *c*-axis (see Fig. 4(2)).

The ζ-$Ta_4C_{3-x}$ phase has a closely packed metal sublattice (see Fig. 4), but the distribution of atoms Ta in this sublattice differs from distributions of metal atoms in FCC and HCP sublattices of cubic carbide $TaC_y$ and hexagonal lower carbide $Ta_2C$. The metal sublattice of the ζ-$Ta_4C_{3-x}$ phase is made up of alternating blocks, in which metal atoms are located both in FCC and HCP sublattices of cubic and hexagonal carbides $TaC_y$ and $Ta_2C$ (see Figs. 4(3) and (4)). It represents a transition structure between the last sublattices. The sequence of metal atomic layers perpendicular to the *c*-axis is ABABCA-CABCBC [10].

The neutron diffraction pattern of carbide $TaC_{0.685}$ contained ζ-$Ta_4C_{3-x}$ phase is shown in Fig. 5. The neutron diffraction pattern was analyzed using the model of a trigonal (space group $R\bar{3}m$) unit cell. The parameters of that cell were determined from the XRD patterns. In an ideal (without atomic displacements) ζ-$Ta_4C_{3-x}$ phase ordering primarily causes an increase of the intensity of reflections from the families of atomic planes, in which atoms C are occupied 3(*a*) sites. As compared with the diffraction pattern of the disordered phase, the reflections (003) and (009) are enhanced in the neutron diffraction pattern of the ordered phase. The reflection (006) is due to the diffraction from the planes occupied by carbon atoms C in positions 6(*c*) only, while the reflection (0012) is the result of diffraction from planes, filled by Ta atoms only. Therefore, the intensities of both reflections remain unchanged while ordering.

Considerable atomic displacements from sites of the ideal lattice take place in a real ζ-phase and, for this reason, the redistribution of the reflection intensities in this case is more complicated. In the neutron diffraction experiment, characteristic evidence to ζ-$Ta_4C_{3-x}$ ordering is the ratio of intensities $I$ of the adjacent reflections (101), (104), (0012), (10−5) and (107) along with the intensification of (009) reflection. The intensity of reflection (101) for the disordered phase is nearly 30 times larger than that for the ordered phase (see Fig. 5, inset). The intensity $I$ of the reflection (104) for the ordered and disordered phases was the same. If the intensity $I_{(104)}$ is assumed to be unity, then the intensities $I_{(0012)} \approx 0.36$, $I_{(10-5)} \approx 0.54$ and $I_{(107)} \approx 17.4$ for the ordered ζ-phase and $I_{(0012)} \approx 0.35$, $I_{(10-5)} \approx 1.30$ and $I_{(107)} \approx 16.1$ for the disordered phase. It should be noted that the experiment showed the intensity $I_{(10-5)}$ was 1.5 times larger than $I_{(0012)}$ (Fig. 5). This situation is characteristic for an ordered phase. Really, taking into account the ordering of the carbon atoms and vacancies in ζ-$Ta_4C_{3-x}$ phase led to the decreasing of $R_I$ value from 0.086 to 0.059 and to the satisfactory coincidence with the experimental neutron diffraction pattern (see Fig. 5). According to the refinement of neutron diffraction pattern, the occupancy numbers for the sites 3(*a*) and 3(*b*) are equal to 0.675(6) and 0, respectively. Thus, calculation generally demonstrated that the experimental neutron diffraction pattern corresponds to the ordered carbide ζ-$Ta_4C_{3-x}$ with $x \approx 0.324$ (or $TaC_{0.669}$). In this ordered ζ-$Ta_4C_{3-x}$ phase carbon atoms occupy only the sites 6(*c*) and 3(*a*) and the sites 3(*b*) are fully vacant as shown in Fig. 4(1).

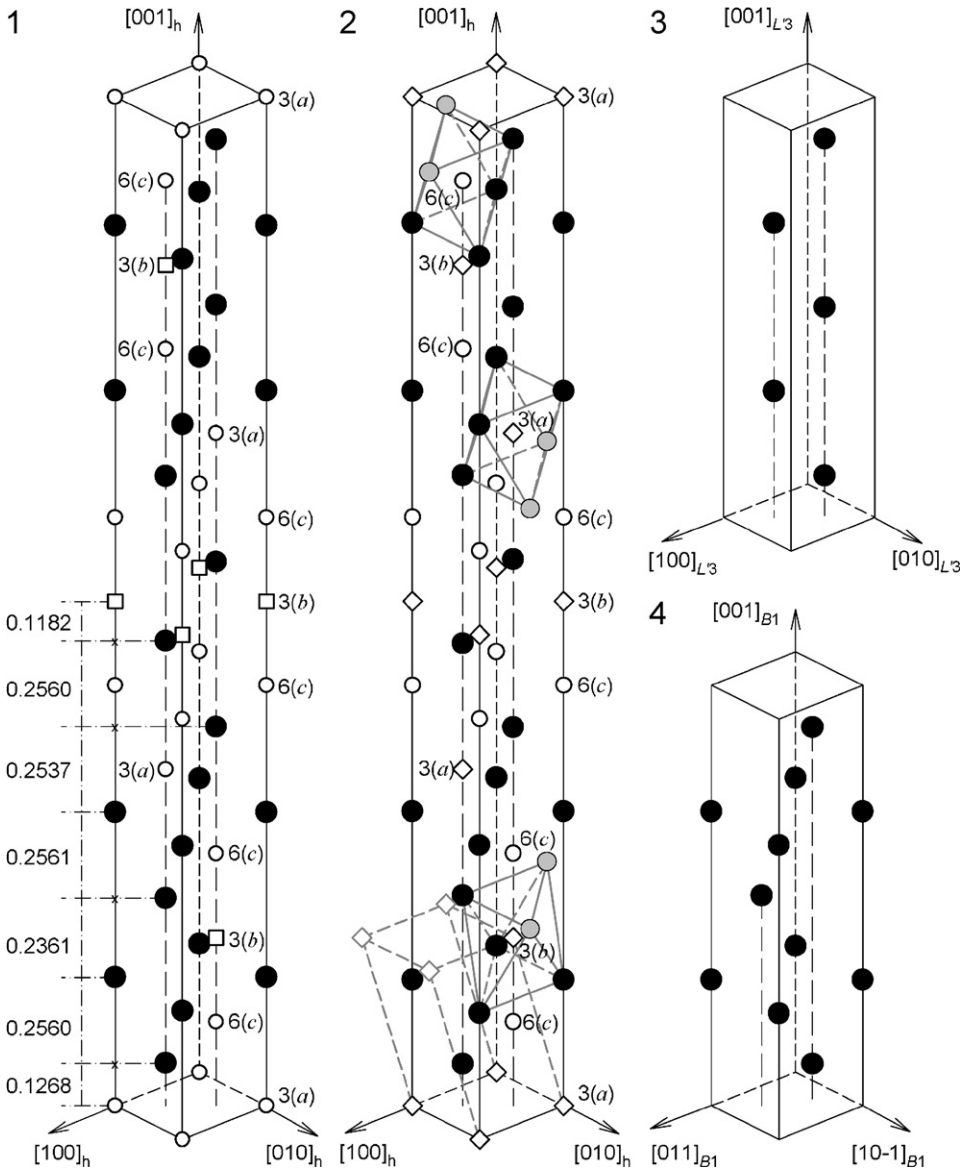


Fig. 4. Distribution of atoms in a unit cell of the trigonal (space group $R\bar{3}m$) ζ-$Ta_4C_{3-x}$ phase (the cell is shown in hexagonal axes, interplanar spacings along the *c*-axis are given in nm). (1) an ordered distribution of carbon atoms C in sites 3(*a*) and structural vacancies □ in sites 3(*b*). (2) in the case of a disordered distribution, carbon atoms and vacancies statistically occupy sites 3(*a*) and 3(*b*) in the nonmetal sublattice with the probability $(1-x)/2$; in addition primitive cell with respect to the nonmetal sites 3(*a*) and 3(*b*) of disordered ζ-phase is shown by dotted gray line; octahedral surrounding of the nonmetal sites 3(*a*), 3(*b*) and 6(*c*) by tantalum atoms is shown for the disordered ζ-$Ta_4C_{3-x}$ phase. (3) and (4) distributions of Ta atoms in the lattices of lower hexagonal carbide $Ta_2C$ with the *L*′3 structure and cubic carbide $TaC_y$ with the *B*1 structure, respectively. (●) atoms Ta; (●) atoms Ta located outside the unit cell; (○) atoms C; (□) structural vacancies; (◇) positions 3(*a*) and 3(*b*) in the nonmetal sublattice statistically occupied by atoms C with the probability $(1-x)/2$.

### 3.2. Distribution function of carbon atoms in carbide ζ-$Ta_4C_{3-x}$

Let us perform the symmetry analysis of ordering in ζ-$Ta_4C_{3-x}$ phase, i.e. establish channel of the disorder–order transition and calculate the distribution function of carbon atom.

A homogeneous distribution of atoms at crystal lattice sites **r** in a disordered ζ-phase is subject to space-periodic modulation during the disorder–order phase transition. The space-periodic modulation of the atomic distribution (deviation of the probability $n(\mathbf{r})$ from its value in the case of a statistical distribution) can be presented as a superposition of several plane concentration waves [22]. The vectors of these waves are the superstructure vectors $\mathbf{k}_s^{(j)}$ of a reciprocal lattice. They are located in the first Brillouin zone of a disordered lattice. In terms of the static concentration waves method [22], the distribution function of atoms of a given species is described by the fraction of sites, *y*, occupied by these atoms and the superposition of static concentration waves

$$n(\mathbf{r}) = y + \sum_s \sum_{j \in s} \Delta(\mathbf{k}_s^{(j)}, \mathbf{r}), \quad (1)$$

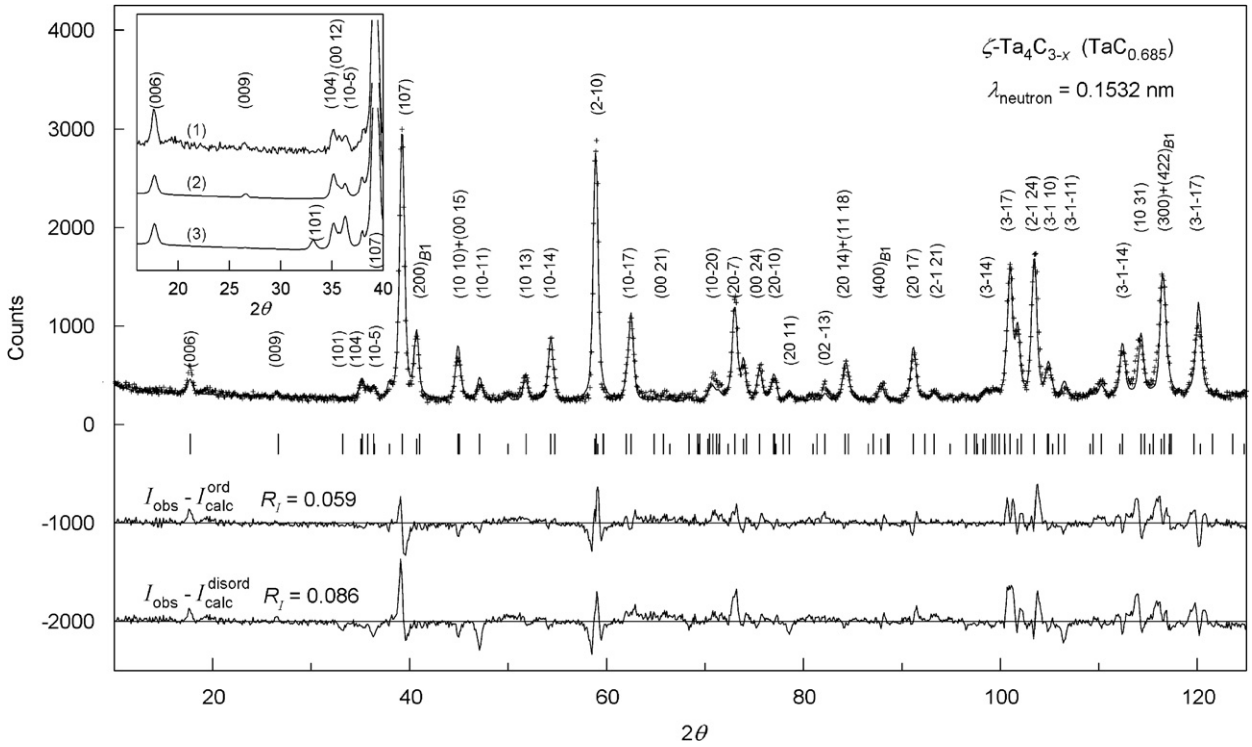


Fig. 5. Observed (crosses), calculated (solid line) and difference neutron diffraction patterns ($\lambda = 0.1532$ nm) of tantalum carbide $TaC_{0.685}$ containing ~75 wt% of the ζ-$Ta_4C_{3-x}$ ($TaC_{0.67}$). The inset presents a fragment of an experimental neutron diffraction pattern (1) in comparison with calculated neutron diffraction patterns of carbide ζ-$Ta_4C_{3-x}$ ($TaC_{0.67}$) phase with ordered (2) and disordered (3) distributions of atoms C and vacancies □ over positions 3(*a*) and 3(*b*) in the nonmetal sublattice. Refining the distribution of atoms C and vacancies □ is lowered the *R* values. Long, middle and short ticks correspond to reflections of ζ-$Ta_4C_{3-x}$, $TaC_{0.76}$ and $Ta_2C$ phases, respectively.

where

$$\Delta(\mathbf{k}_s^{(j)}, \mathbf{r}) = \tfrac{1}{2}\eta_s\gamma_s[\exp(\mathrm{i}\varphi_s^{(j)})\exp(\mathrm{i}\mathbf{k}_s^{(j)}\mathbf{r}) + \exp(-\mathrm{i}\varphi_s^{(j)})\exp(-\mathrm{i}\mathbf{k}_s^{(j)}\mathbf{r})] \quad (2)$$

is a standing static plane concentration wave generated by the superstructure vector $\mathbf{k}_s^{(j)}$ of the wave-vector star $\{\mathbf{k}_s\}$. In Eq. (2) $\eta_s\gamma_s$ and $\varphi_s^{(j)}$ stand for the amplitude and the phase shift of a concentration wave, respectively. From Eqs. (1) and (2) it follows that the long-range order parameter $\eta_s$ corresponds to each star $\{\mathbf{k}_s\}$ of the wave vector. The distribution function at sites $\mathbf{r}$ located in crystallographically equivalent positions has an identical value, because it is invariant under rotation and mirror transformations comprising in the point symmetry group of an ordered crystal. The number of values, which the distribution function can assume at sites of an ordered lattice, exceeds the number of long-range order parameters by one. It is shown [1,2] that summation in Eq. (1) is to be taken over all superstructure vectors comprising in the disorder–order phase transition channel. The procedure of calculation of a phase transition channel and the distribution function is described in detail by authors [2].

In ζ-phase under discussion, an ordering Ising lattice is a nonmetal sublattice which is formed by the sites 3(*a*) and 3(*b*) only. One can select a primitive (with respect to the nonmetal sites) translational cell in this sublattice of a disordered ζ-$Ta_4C_{3-x}$ carbide (see Fig. 4(2)). Structure vector $\mathbf{b}_3$ of the reciprocal lattice for the primitive cell is equal to $(006\pi/c_h)$, where $c_h$ is the lattice constant of the trigonal (space group $R\bar{3}m$) ζ-$Ta_4C_{3-x}$ phase along the *c*-axis.

Ordering is caused by the redistribution of carbon atoms C and vacancies at the crystal lattice sites 3(*a*) and 3(*b*) and leads to the doubling of the primitive cell in the direction of *c*-axis. Calculation and translation of the superstructure vectors of the reciprocal lattice show that the first Brillouin zone of the disordered primitive cell includes one nonequivalent superstructure vector corresponding to the ray $\mathbf{k}_{17}^{(1)} = b_3/2$ of the Lifschitz one-ray star $\{\mathbf{k}_{17}\}$ (if ζ-phase is described in hexagonal axes) or to the ray $\mathbf{k}_4^{(1)} = b_3/2$ of the Lifschitz three-ray star $\{\mathbf{k}_4\}$ (at description of ζ-phase in trigonal axes). The arms $\mathbf{k}_s^{(j)}$ and wave-vector star $\{\mathbf{k}_s\}$ of the basic hexagonal and trigonal lattices are numbered and described according to [23]. Thus, ordered phase ζ-$Ta_4C_{3-x}$ is formed through a disorder–order phase transition channel involving one vector $\mathbf{b}_3/2 = (00\frac{1}{2})$ in $6\pi/c_h$ units. Therefore, summation over *s* is omitted in Eq. (1) and the distribution function of carbon atoms C in carbide ζ-$Ta_4C_{3-x}$ depends on one long-range order parameter $\eta$.

Considering an ordered distribution of carbon atoms C and vacancies □ on sites 3(*a*) and 3(*b*), the structural formula of the ζ-phase can be written as $Ta_4C_2C_{1-x}\square_{1+x}$. The perfect ordering with the long-range order parameter

Table 3
Trigonal (space group no. 166, $R\bar{3}m$ ($D_{3d}^5$)) carbide $\zeta$-$Ta_4C_{3-x}$, $Z=3$

| Atom | Site | Atomic coordinates in hexagonal axes $x_h$ | $y_h$ | $z_h$ | $B_{iso}\times10^{-4}$ (pm$^2$) | Occupation number | Values for the distribution function $n$ ($x_h$, $y_h$, $z_h$) |
|---|---|---|---|---|---|---|---|
| C1[a] | 3(*a*)[a] | 0 | 0 | 0 | 1.2(1) | 0.675(6) | $n_2=(1-x)/2+\eta/2$ |
| C2 (vacancy) | 3(*b*) | 0 | 0 | 0.5 | – | 0 | $n_1=(1-x)/2-\eta/2$ |
| C3 | 6(*c*) | 0 | 0 | 0.4169(9) | 0.9(8) | 1 | |
| Ta1 | 6(*c*) | 0 | 0 | 0.1273(6) | 0.65(7) | 1 | |
| Ta2 | 6(*c*) | 0 | 0 | 0.291(10) | 0.57(5) | 1 | |

[a]In carbide $\zeta$-$Ta_4C_{3-x}$ at $x=0$ and the maximum degree of the long-range order carbon atoms C occupy all positions 3(*a*); at $x>0$ and the maximum degree of the long-range order atoms C occupy only some positions 3(*a*), while the other positions 3(*a*) are vacant. Positions 3(*b*) are always vacant irrespectively of the composition and the degree of order, while positions 6(*c*) in the nonmetal sublattice are always occupied with carbon atoms.

$\eta_{max}=1$ is achieved at $x=0$ when all positions 3(*a*) are occupied by atoms C and positions 3(*b*) are vacant. As $x$ increases, i.e. the vacancy concentration enlarges, the value of the parameter $\eta_{max}$ decreases due to vacancies appearance on sites 3(*a*). The dependence of the maximum value of the long-range order parameter on the $\zeta$-phase composition is $\eta_{max}(x)=(1-x)$. In the disordered $\zeta$-phase the positions 3(*a*) and 3(*b*) are occupied by $3(1-x)$ atoms C with equal probability; hence, the relative concentration $y$ of carbon atoms participating in ordering is $(1-x)/2$. Considering this and transition channel found, the distribution function $n(\mathbf{r})$ for carbon atoms was calculated. This function describing the distribution of atoms C on sites 3(*a*) and 3(*b*) of the nonmetal sublattice of the $\zeta$-phase has the following form:

$$n(\mathbf{r})=(1-x)/2+(\eta/2)\cos 6\pi z_h, \quad (3)$$

where $\mathbf{r}=(x_h y_h z_h)$ is the site $(x_h y_h z_h)$ occupying the position 3(*a*) or 3(*b*) of the nonmetal sublattice (the coordinates of the lattice site are written in hexagonal axes). The distribution function (3) represents the probability of the locating carbon atoms on sites $\mathbf{r}$ relevant to positions 3(*a*) and 3(*b*) of the $\zeta$-$Ta_4C_{3-x}$ phase. If the long-range order $\eta_{max}(x)=(1-x)$ is a maximum, the function (3) takes the value $(1-x)$ on all sites 3(*a*) and it is equal to 0 on sites 3(*b*). In other words, if the long-range order is a maximum, the probability of finding an atom C on sites 3(*a*) is $(1-x)$ and on sites 3(*b*) is equal to 0. In the absence of the order, when $\eta=0$, the distribution function $n(r)$ is equal to $(1-x)/2$ on all sites 3(*a*) and 3(*b*). Values of the distribution function (3) on sites 3(*a*) and 3(*b*) of the nonmetal sublattice of the $\zeta$-$Ta_4C_{3-x}$ phase are given in Table 3.

According to the lattice site occupancies obtained (see Table 3), the composition of $\zeta$-phase corresponds to $\sim TaC_{0.669}$ or $Ta_4C_{3-x}$ with $x\approx0.324$. In this case, from the above analysis it follows that the long-range order parameter $\eta$ in the investigated $\zeta$-$Ta_4C_{3-x}$ phase does not exceed $\sim0.7$.

Fig. 6 presents the static concentration wave calculated for the nonmetal plane $(20-1)_{hex}$ in ordered trigonal (space group $R\bar{3}m$) $\zeta$-$Ta_4C_{3-x}$ phase. The maxima and minima of the concentration wave correspond to the intersections of plane $(20-1)$ by the nonmetal planes $(00l)$ which are formed by the occupied 3(*a*) sites and vacant 3(*b*) sites, respectively.

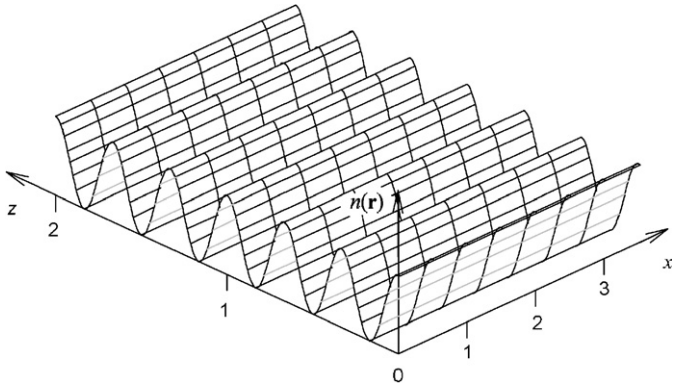


Fig. 6. Concentration wave in the nonmetal plane $(20-1)_{hex}$ of ordered trigonal (space group $R\bar{3}m$) $\zeta$-$Ta_4C_{3-x}$ phase. The maxima and minima of this concentration wave correspond to the nonmetal planes $(00l)$ which are formed by the occupied 3(*a*) sites and vacant 3(*b*) sites, respectively.

In principle, if $x>0$, the distribution of carbon atoms and vacancies on the 3(*a*) positions may be disordered or ordered too. If this ordering exists, additional superstructure reflections should appear in the neutron diffraction pattern at small angles $2\theta<30^\circ$. Additional reflections were not detected in the experiment and, therefore, one may suppose that the statistical distribution of atoms C and vacancies □ on sites 3(*a*) is realized in the $\zeta$-$Ta_4C_{3-x}$ ($TaC_{0.67}$) phase under study.

## 4. Phase diagram of the Ta–C system

The equilibrium phase diagram of the Ta–C system, which takes into account atomic ordering in nonstoichiometric cubic tantalum carbide $TaC_y$, was calculated earlier [1,2] using the order parameter functional (OPF) method. The study of the structure of the $\zeta$-$Ta_4C_{3-x}$ phase allowed determining more precisely the temperature and concentration boundaries of its range in the phase diagram of the Ta–C system. The constructed phase diagram of the Ta–C system is shown in Fig. 7. The position of the phase

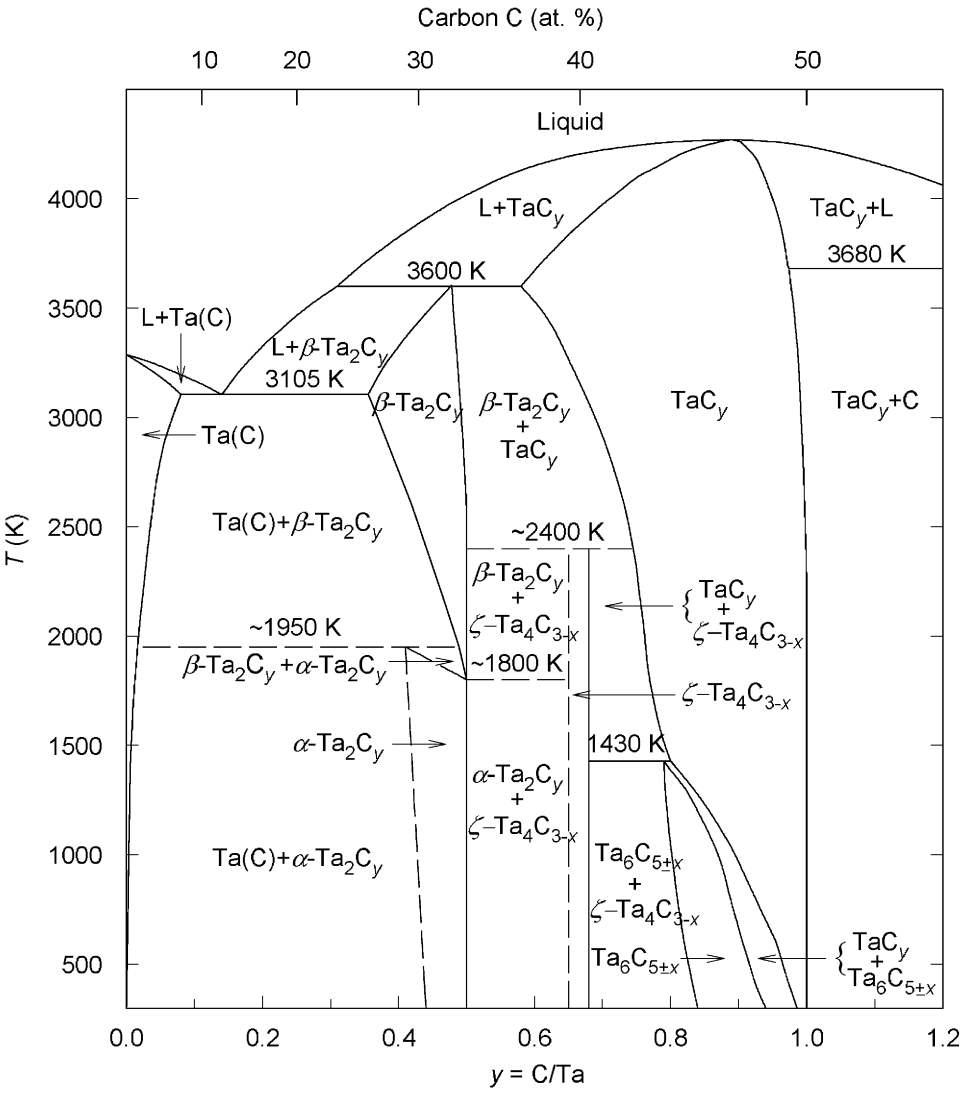


Fig. 7. Equilibrium phase diagram of the Ta–C system taking into account atomic ordering in nonstoichiometric cubic tantalum carbide $TaC_y$. The position of the trigonal (rhombohedral) ζ-$Ta_4C_{3-x}$ phase is shown in accordance with the obtained experimental results and literature data. This phase is not an ordered phase of carbide $TaC_y$ and exists in a wide temperature interval of ~2400–300 K. Ta(C) is interstitial solid solution of carbon in tantalum.

boundaries outside the ordering region of cubic carbide $TaC_y$ is given in accordance with handbook [24].

The ζ-$Ta_4C_{3-x}$ phase is not an ordered phase of carbide $TaC_y$ since it has its own (trigonal and not cubic) metal sublattice. According to [13,14], heating of $TaC_{0.71}$ and $TaC_{0.76}$ samples contained the ζ-phase at 1270–1470 K led to vanishing of the ζ-phase. Moreover, according to the data [14] grinding of carbide $TaC_{0.76}$ led to vanishing of the ζ-phase also. This effect was observed earlier by Zaplatinsky [7]. Apparently, in studies [7,10,13,14] the ζ-phase was obtained in the nonequilibrium state and, therefore, annealing or grinding of the bulk samples led to its transformation to cubic carbide $TaC_y$. According to the data [15] obtained by the diffusion couples method, the ζ-phase has a very narrow homogeneity interval (the carbon content of 38.2–39.0 at%), appears at a temperature below 2450 K, and is not detected at $T<1400$ K. However, the diffusion couples method is not thermodynamically equilibrium since test samples have a concentration gradient of their components over the cross-section. The conclusions [13–15] about a limited interval of the thermal stability of ζ-$Ta_4C_{3-x}$ contradict the experimental data [16,17] and results of the present study. Specifically, this study revealed that carbide ζ-$Ta_4C_{3-x}$ was stable in the bulk and powdered states in a wide temperature interval of 300–~2400 K and its composition in the investigated samples is close to $TaC_{0.67-0.68}$. Taking into account the literature data [11,16,17] and results of this study, one may suppose that trigonal carbide ζ-$Ta_4C_{3-x}$ has a narrow homogeneity interval from $TaC_{0.65}$ to $TaC_{0.68}$ and exists at a temperature from ~2400 to 300 K.

It is seen from Fig. 7 that the $Ta_6C_{5\pm x}$ phase is the only ordered phase of nonstoichiometric cubic tantalum carbide $TaC_y$. Indeed, neutron diffraction analysis of the structure

of ordered tantalum carbide [19,25] showed that an incommensurate ordered phase similar to known $M_6C_5$ superstructures is formed in nonstoichiometric cubic tantalum carbide $TaC_y$. To produce ordered phase $Ta_6C_{5\pm x}$ the samples synthesized were annealed at a temperature 1600 K with following slow cooling to 750 K at a rate of 0.15–0.25 K $min^{-1}$. A study of magnetic susceptibility [26] also confirmed the formation of an ordered phase like $M_6C_5$ in tantalum carbide. The temperature $T_{trans}$ of the $Ta_6C_{5\pm x}$–$TaC_y$ transition, which was determined from magnetic susceptibility measurements, is equal to 1110 and 1130 K for carbides $TaC_{0.83}$ and $TaC_{0.85}$. These values are in good agreement with $T_{trans}$ values calculated in this study by the OPF method [1,2] for phase transformations related to ordering in cubic carbide $TaC_y$ (Table 4).

Table 4
Thermodynamic characteristics of order–disorder phase transitions $Ta_6C_{5\pm x}$–$TaC_y$ in nonstoichiometric tantalum carbide $TaC_y$

| $y$ | $T_{trans}$ (K) | $\Delta S_{trans}$ (J $mol^{-1}$ $K^{-1}$) | $\Delta H_{trans}$ (kJ $mol^{-1}$) |
|---|---|---|---|
| 0.80 | 1399 | 1.10 | 1.54 |
| 0.82 | 1325 | 1.22 | 1.61 |
| 0.833 | 1270 | 1.26 | 1.60 |
| 0.84 | 1239 | 1.28 | 1.58 |
| 0.85 | 1190 | 1.28 | 1.52 |
| 0.86 | 1137 | 1.26 | 1.43 |
| 0.88 | 1020 | 1.15 | 1.17 |
| 0.90 | 887 | 0.98 | 0.87 |
| 0.92 | 738 | 0.79 | 0.58 |
| 0.94 | 576 | 0.58 | 0.34 |
| 0.95 | 489 | 0.49 | 0.24 |

## 5. Microhardness of tantalum carbides $TaC_y$ and $\zeta$-$Ta_4C_{3-x}$

The microhardness $H_V$ of nonstoichiometric tantalum carbides $TaC_y$ with the basic cubic structure $B1$ and trigonal phase $\zeta$-$Ta_4C_{3-x}$ was measured using samples prepared by solid-phase vacuum sintering of compacted powder mixtures of Ta and carbon black. The synthesized samples were quenched to bring them reliably to a disordered state and annealed to achieve an ordered state. The porosity of the sintered $TaC_y$ samples was 15–16% for nearly stoichiometric carbides $TaC_{0.96–1.00}$ and up to 8% for carbides $TaC_{0.70–0.75}$ near the low boundary of the homogeneity interval of the cubic phase with the $B1$ structure. The grain size was 10–20 μm on the average. According to the data [19,25] an incommensurate ordered phase like $M_6C_5$ is formed over the composition region $TaC_{0.79}$–$TaC_{0.89}$.

The microhardness $H_V$ of the annealed $TaC_y$ samples that exhibit superstructure reflections in the neutron diffraction patterns [19,25] is a little larger than $H_V$ of the quenched disordered $TaC_y$ samples, but this difference does not exceed the measurement error (Fig. 8).

As the tantalum carbide composition changes from $TaC_{1.00}$ to $TaC_{0.85}$, the microhardness increases from 21 to 23–24 GPa, reaches a maximum for carbide $TaC_{0.83–0.85}$ and then decreases to 21 GPa at the lower boundary of the homogeneity interval of cubic tantalum carbide $TaC_y$. The presence of the maximum in the obtained dependence $H_V(y)$ of tantalum carbide is in agreement with the literature data [27,28]. The explanation for this maximum is that over the $TaC_{0.81}$–$TaC_{0.87}$ range plastic deformation is due predominantly to the slip system {100} ⟨110⟩, which requires higher stresses, while the role of the slip system {111} ⟨110⟩, which is connected mostly with $M$–$M$ interactions, becomes less significant in the series from

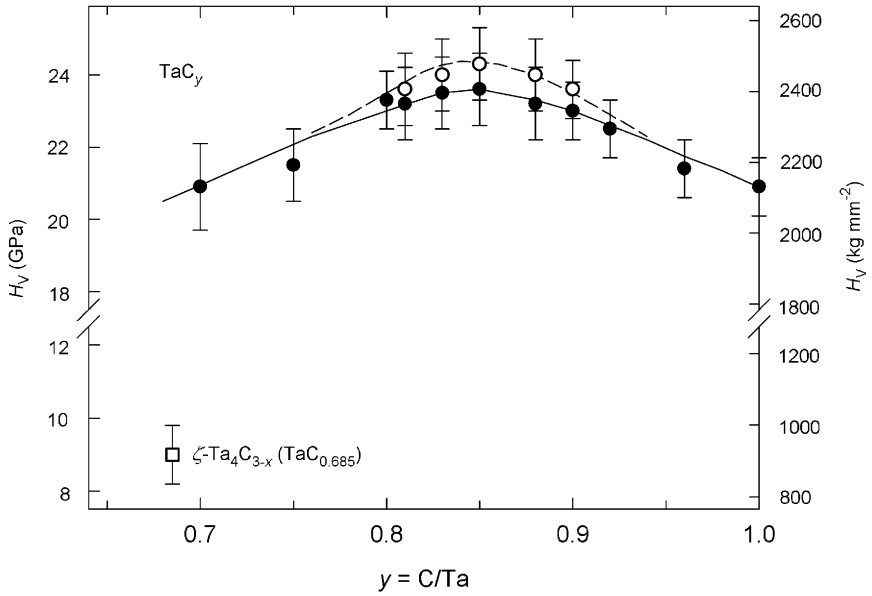


Fig. 8. Microhardness $H_V$ of tantalum carbide: (●) quenched disordered and (○) annealed ordered carbide $TaC_y$ with the basic cubic structure $B1$; (□) tantalum carbide $TaC_{0.685}$ containing ~75 wt% of the trigonal (rhombohedral) carbide $\zeta$-$Ta_4C_{3-x}$ ($TaC_{0.67}$).

$TaC_{1.00}$ to $TaC_{0.81–0.85}$. Indeed, the high-energy $M–M$ band in the electron energy spectrum is less than half-filled even in stoichiometric carbide $TaC_{1.00}$ [2]. If the carbide composition deviates from stoichiometry, the occupancy of the $M–M$ band decreases, and the band becomes almost empty in carbide $TaC_{0.81–0.83}$, while the relative contribution of covalent Ta–C interactions increases. The enhancement of the covalent component and weakening of the metal component of the combined chemical bond in $TaC_y$ show up as the increase in $H_V$ values as the carbide composition changes from $TaC_{1.00}$ to $TaC_{0.85}$. When the carbon content decreases further over the interval of compositions from $TaC_{0.85}$ to $TaC_{0.70}$, the occupancy of the $M–M$ band diminishes, leading to weakening of the covalent component of the chemical bond. This shows up as a smooth decrease in the microhardness.

It is seen from Fig. 8 that annealing effect on the microhardness of $TaC_y$ carbide is weak. The domain size of the ordered incommensurate phase forming in annealed carbide $TaC_y$ is equal to ~200 nm and is smaller than the size of grains in the disordered basic (parent) phase. However, the degree of the long-range order, which was achieved in the ordered phase after annealing, was much smaller than the maximum degree. Indeed, according to the estimates [1,2], which were made using measured values of the basic lattice constant $a_{B1}$, the heat capacity $C_p$ and the magnetic susceptibility $\chi$, the long-range order parameter in carbides $TaC_{0.81}$–$TaC_{0.88}$ does not exceed 0.6–0.7, i.e. $\eta = \eta_{trans}$ at the disorder–order transition point. This is probably one of the reasons for the weak effect of annealing on the microhardness of tantalum carbide.

The microhardness $H_V$ of the sintered tantalum carbide $TaC_{0.685}$ containing ~75 wt% of the trigonal $\zeta$-$Ta_4C_{3-x}$ ($TaC_{0.67}$) phase is ~9 GPa, i.e. more than 2 times smaller than $H_V$ of disordered cubic carbide $TaC_{0.70}$ having the closest composition (see Fig. 8). According to the data [17], the microhardness of the $\zeta$-$Ta_4C_{3-x}$ phase does not exceed 11 GPa. The fact that the microhardness of the $\zeta$-phase is much smaller than the microhardness of cubic tantalum carbide is due primarily to its structure, in which a significant role is imparted to stacking faults. Considering the $\zeta$-phase structure, its microhardness most likely should be anisotropic. However, this property could not be detected in the polycrystalline sample of $TaC_{0.67}$.

## 6. Conclusion

Generally, results of this study demonstrated that carbide $\zeta$-$Ta_4C_{3-x}$ represents an individual nonstoichiometric compound of the Ta–C system along with other two nonstoichiometric compounds, namely hexagonal $Ta_2C_y$ and cubic $TaC_y$ carbides. Carbide $\zeta$-$Ta_4C_{3-x}$ is stable in bulk and powdered states over a wide temperature interval of 300 to ~2400 K and has a narrow homogeneity interval from $TaC_{0.65}$ to $TaC_{0.68}$. Carbide $\zeta$-$Ta_4C_{3-x}$ has the trigonal (space group $R\bar{3}m$) symmetry with ordering in the nonmetal sublattice. The ordering in $\zeta$-$Ta_4C_{3-x}$ carbide is described by one long-range order parameter $\eta$: if $x = 0$ and the degree of the long-range order is a maximum, carbon atoms C occupy all sites 3($a$), while sites 3($b$) are fully empty; if $x > 0$ and the degree of the long-range order is a maximum, atoms C occupy some sites 3($a$), while vacancies occupy all sites 3($b$) and some sites 3($a$). The closely packed metal sublattice of the $\zeta$-$Ta_4C_{3-x}$ phase is a transition between metal sublattices of cubic $TaC_y$ and hexagonal $Ta_2C$ carbides.

## Acknowledgments

The authors are indebted to the Russian Foundation for Basic Research (Grant no. 06-03-32047) for financial support.

## References

[1] A.I. Gusev, Nonstoichiometry, Disorder, Short-Range and Long-Range Order in Solids, Nauka-Fizmatlit, Moscow, 2007 (in Russian).
[2] A.I. Gusev, A.A. Rempel, A.J. Magerl, Disorder and Order in Strongly Nonstoichiometric Compounds. Transition Metal Carbides, Nitrides and Oxides, Springer, Berlin, Heidelberg, New York, London, 2001.
[3] R. Lesser, G. Brauer, Z. Metallkd. 49 (1958) 622–626.
[4] E. Rudy, H. Nowotny, Monatsh. Chem. 94 (1963) 507–517.
[5] E. Rudy, F. Benesovsky, L. Toth, Z. Metallkd. 54 (1963) 345–353.
[6] E. Rudy, D.P. Harmon, Partial investigation in the systems Nb–C and Ta–C, in: Ternary Phase Equilibria in Transition Metal–Boron–Carbon–Silicon Systems: Part I. Related Binary Systems, Technical Report AFML-TR-65-2, vol. V, Wright-Patterson Air Force Base, Metals and Ceramics Division, Air Force Materials Laboratory, OH, 1965, pp. 1–78.
[7] I. Zaplatinsky, J. Am. Ceram. Soc. 49 (1966) 109–110.
[8] W.F. Brizes, J.M. Tobin, J. Am. Ceram. Soc. 50 (1967) 115–116.
[9] G.J. Santoro, H.B. Probst, Explanation of microstructure in the Ta–C system, in: W.M. Mueller, M. Fay (Eds.), Advances in X-ray Analysis, vol. 7, Plenum Press, New York, 1964, pp. 126–134.
[10] K. Yvon, E. Parthe, Acta Crystallogr. B 26 (1970) 149–152.
[11] J.L. Martin, A. Rocher, B. Jouffrey, P. Costa, Philos. Mag. 24 (1971) 1355–1364.
[12] D.J. Rowcliffe, G. Thomas, Mater. Sci. Eng. 18 (1975) 231–238.
[13] B.I. Markhasev, N. Ch. Pioro, V.V. Klyugvant, Yu.L. Pilipovskii, Yu.M. Shamatov, E.I. Geshko, Izv. AN SSSR. Neorgan. Mater. 19 (1983) 1997–2000 (in Russian).
[14] B.I. Markhasev, N.Ch. Pioro, V.V. Klyugvant, Yu.L. Pilipovskii, Yu.M. Shamatov, E.I. Geshko, Izv. AN SSSR. Neorgan. Mater. 18 (1982) 2001–2004 (in Russian).
[15] H. Wiesenberger, W. Lengauer, P. Ettmayer, Acta Mater. 46 (1998) 651–656.
[16] G.M. Demyashev, M.A. Khusainov, R.K. Chuzhko, Izv. AN SSSR. Seriya Fizicheskaya 48 (1984) 1693–1696 (in Russian).
[17] M.A. Khusainov, G.M. Demyashev, M.M. Myshlyaev, Russian Metallurgy No 5 (1990) 139–141.
[18] A.I. Gusev, V.N. Lipatnikov, JETP Lett. 82 (2005) 287–291.
[19] A.I. Gusev, A.A. Rempel, V.N. Lipatnikov, J. Phys.: Condens. Matter 8 (1996) 8277–8293.
[20] A. Altomare, M.C. Burla, M. Camalli, B. Carrozzini, G.L. Cascarano, C. Giacovazzo, A. Guagliardi, A.G.G. Moliterni, G. Polidori, R. Rizzi, J. Appl. Crystallogr. 32 (1999) 339–340.

[21] A.C. Larson, R.B. von Dreele, General Structure Analysis System (GSAS), Los Alamos National Laboratory Report LAUR 86-748. Los Alamos, 2004, 231pp.
[22] A.G. Khachaturian, Theory of Structural Transformations in Solids, Wiley, New York, 1983.
[23] O.V. Kovalev, Representations of the Crystallographic Space Groups: Irreducible Representations, Induced Representations and Corepresentation, Gordon & Breach Science Publishers, Yverdon—Paris, Berlin—London, Tokyo, Amsterdam, 1993, 390pp.
[24] A.E. McHale (Ed.), Phase Equilibria Diagrams. Phase Diagrams for Ceramists,, vol. X, American Ceramic Society Publishers, Westerville (OH), 1994, pp. 265–268.
[25] V.N. Lipatnikov, A.A. Rempel, JETP Lett. 81 (2005) 326–330.
[26] A.I. Gusev, A.A. Rempel, V.N. Lipatnikov, Phys. Stat. Sol. A 106 (1988) 459–466.
[27] G. Santoro, Trans. Met. Soc. AIME 227 (1963) 1361–1368.
[28] L. Ramqvist, Jernkontorets Annaler 152 (1968) 467–475.